

Review of cardiovascular imaging in the Journal of Nuclear Cardiology 2018. Part 1 of 2: Positron emission tomography, computed tomography, and magnetic resonance

Wael A. AlJaroudi, MD, FASNC,^a and Fadi G. Hage, MD, MASNC^{b,c}

^a Division of Cardiovascular Medicine, Clemenceau Medical Center, Beirut, Lebanon

^b Division of Cardiovascular Disease, Department of Medicine, University of Alabama at Birmingham, Birmingham, AL

^c Section of Cardiology, Birmingham Veterans Affairs Medical Center, Birmingham, AL

Received Nov 28, 2018; accepted Nov 28, 2018

doi:10.1007/s12350-018-01558-y

In this review, we summarize key articles that have been published in the Journal of Nuclear Cardiology in 2018 pertaining to nuclear cardiology with advanced multi-modality and hybrid imaging including positron emission tomography, cardiac-computed tomography, and magnetic resonance. In an upcoming review, we will summarize key articles that relate to the progress made in the field of single-photon emission computed tomography. We hope that these sister reviews will be useful to the reader to navigate the literature in our field. (J Nucl Cardiol 2019;26:524–35.)

Key Words: CAD • heart Failure • sarcoid heart disease • amyloid heart disease • inflammation • metabolic

Several original articles and accompanying editorials have been published in the Journal of Nuclear Cardiology in 2018. Similar to prior years,^{1–8} it has become a tradition at the beginning of each year to summarize some of these key articles in 2 sister reviews. This first part will discuss some of the progress made in nuclear cardiology with advanced multi-modality and hybrid imaging including positron emission tomography (PET), cardiac-computed tomography (CT), and magnetic resonance (CMR). The second part will focus on progress made in the field of single-photon emission computed tomography (SPECT).

INFLAMMATION

Atherosclerosis is an active inflammatory process that results in oxidation of low-density lipoprotein and plaque formation with focal sites of calcification.⁹ The quest to identify atherosclerotic plaques, particularly vulnerable ones at risk of rupture, is constantly evolving.¹⁰ 18F-Sodium Fluoride (NaF) is a new PET tracer that is taken up at the sites of calcification and ossification due to physicochemical exchange of 18F ion with hydroxyl group in hydroxyapatite deposited at such locations. As such, it has been used successfully in identifying inflamed plaques with incremental value to 18F-FluoroDeoxyGlucose (FDG).¹¹

The process of atherosclerosis starts early in life; age, male gender, family history, smoking, and other cardiovascular risk factors are associated with early plaque development. Ferreira et al evaluated 25 patients without known cardiovascular disease that underwent 18F-NaF PET imaging.¹² The mean target-to-background ratio (max standardized uptake value [SUV]/mean blood-pool SUV) was higher in men than in women, and the corrected uptake per lesion was higher

Reprint requests: Fadi G. Hage, MD, MASNC, Division of Cardiovascular Disease, Department of Medicine, University of Alabama at Birmingham, 306 Lyons-Harrison Research Building, 701 19th Street South, Birmingham, AL 35294-0007; fadihage@uab.edu
1071-3581/\$34.00

Copyright © 2019 American Society of Nuclear Cardiology.

in patients with 3 or more cardiovascular risk factors. Hence, ^{18}F -NaF PET imaging might prove useful in identifying early inflammatory plaques, guiding prevention strategies, and tailoring treatment. These results, however, remain hypothesis generating, pending validation studies.

In another study, Marchesseau et al performed hybrid PET/CT and PET/CMR studies on 10 patients with ST-elevation myocardial infarction. There was higher target-to-background ratio in the culprit coronary artery lesions versus non-culprit lesions (2.11 ± 0.45 vs 1.46 ± 0.48 ; $P < 0.001$), which highlights the role of ^{18}F -NaF PET imaging in identifying ruptured and eroded coronary artery plaques¹³ (Figure 1). The identification of culprit plaques in patients with acute coronary syndrome is not an easy task.¹⁴ Also, the

accurate quantification of plaque imaging using ^{18}F -NaF PET requires partial volume correction, which was recently shown to improve lesion-to-background ratio of both calcified and non-calcified plaques, in both phantom and clinical patients studies.¹⁵ Other potential confounding issues in examining coronary arteries and plaques with PET imaging relates to the low spatial resolution of the obtained images, and the combined cardiac and respiratory motions during data acquisition over several minutes. While many challenges still exist with plaque imaging, the field and technology is constantly evolving (see section on Technical Aspect of Imaging at the end of this review).¹⁶

Although ^{18}F -NaF PET has been used mainly for plaque imaging, the study by Marchesseau et al showed that there was also increased tracer uptake in the

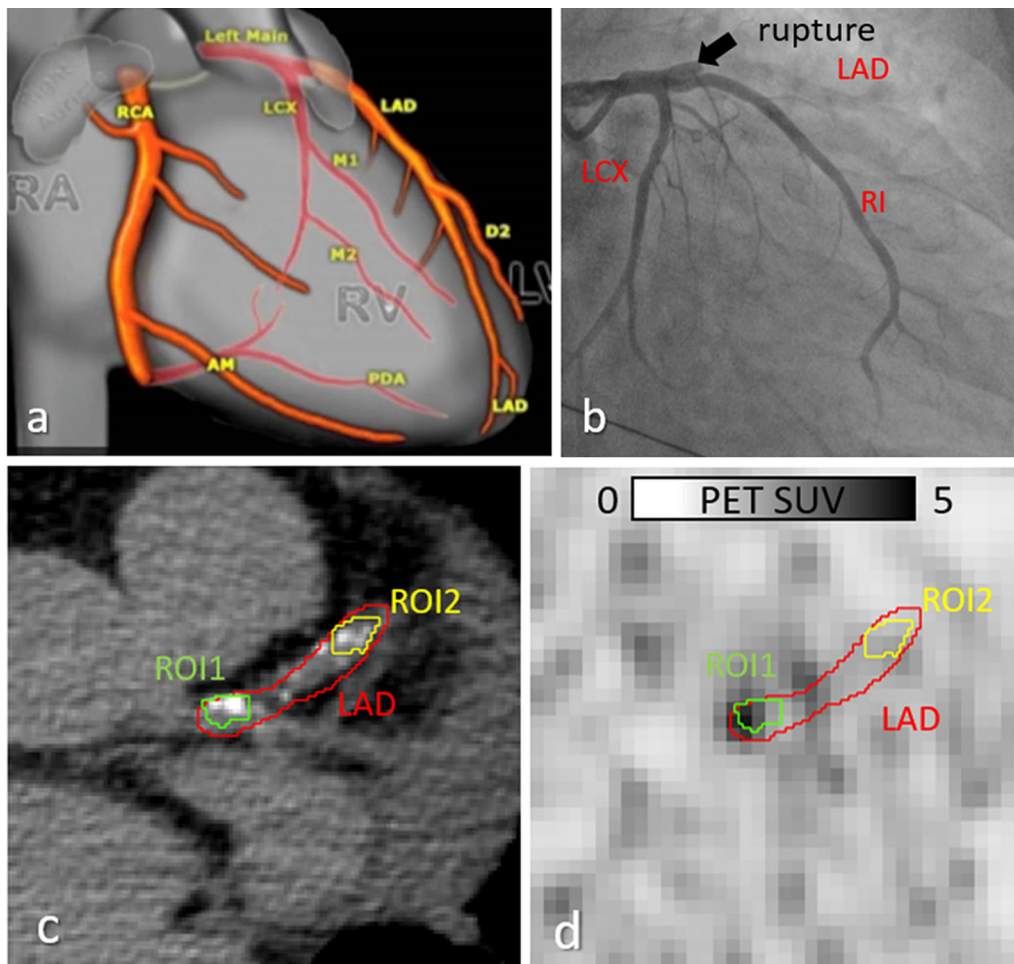


Figure 1. Illustrative case of hybrid ^{18}F -NaF PET-CT imaging. **A** represents normal coronary anatomy. Coronary angiogram shows occluded proximal LAD (left anterior descending coronary artery, **B**) in a patient with ST-elevation myocardial infarction. Several partially calcified plaques are seen on the CT in the LAD vessel (**C**), with increased standardized uptake value of ^{18}F -NaF tracer at the site of ruptured plaque (**D**). Reproduced with permission from Marchesseau et al¹³.

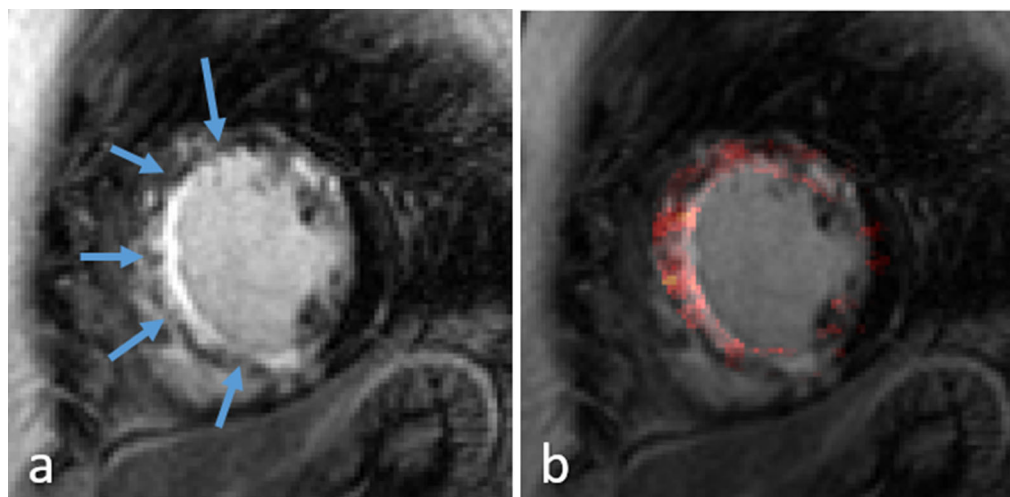


Figure 2. Illustrative case showing increased ^{18}F -NaF uptake within the infarcted myocardium (right panel, red signal) with similar distribution of late gadolinium enhancement with cardiac magnetic resonance (left panel, blue arrow). Reproduced with permission from Marchesseau et al¹³.

infarcted myocardium, which was also confirmed by PET/CMR through increased late gadolinium enhancement¹³ (Figure 2). Hence, a new potential application for ^{18}F -NaF PET imaging is identifying myocardial inflammation and scar formation.

^{18}F -FDG is a more established PET tracer for the assessment of hot plaques¹⁷ as well as inflamed myocardium, particularly cardiac nodules in sarcoidosis.^{18–20} Myocarditis is another inflammatory process that could potentially be assessed with ^{18}F -FDG-PET imaging. Indeed, Nensa et al enrolled 65 patients with suspected myocarditis and performed simultaneous CMR and ^{18}F -FDG-PET imaging.²¹ T2-weighted imaging and late Gadolinium enhancement were performed with the CMR for edema and inflammation/scar quantification, respectively. Ten patients were excluded; two patients had claustrophobia and could not undergo CMR; eight patients had suboptimal PET images due to failed inhibition of myocardial glucose uptake. Compared with CMR (used as gold standard), the sensitivity and specificity of PET was 74% and 97%, respectively, and with overall moderate spatial agreement between imaging modalities $\kappa = 0.73$. While ^{18}F -FDG-PET imaging seems an attractive modality for diagnosing myocarditis, Rischpler et al nicely pointed out in an accompanying editorial that around 12% of the studies were uninterpretable because of physiologic uptake of ^{18}F -FDG by normal cardiomyocytes; this poses a significant limitation, and explains the modest correlation with CMR that remains the gold standard.²² Novel PET tracers that exclusively target inflammatory mechanisms are warranted and should be evaluated in

this setting.²³ Also, studies involving serial imaging with PET to guide and monitor treatment, as well as risk stratify and provide prognostic data, are needed. Still, this remains the first paper to evaluate the role of hybrid ^{18}F -FDG-PET/CMR imaging in myocarditis, paving the way to further studies and novel tracers.²¹

Similar to myocardial inflammation, muscular inflammation with tissue injury secondary to atheroembolic cholesterol crystal showering in patients with peripheral vascular disease, has been recently studied using PET imaging. Pervaiz et al performed ^{18}F -FDG-PET imaging on rabbits that underwent intra-arterial injection of cholesterol crystal ($n = 10$), polystyrene microspheres ($n = 5$), or normal saline ($n = 7$). Despite normal arterial flow with CT angiography, myocardial injury was detected in the first group as reflected by increased creatinine phosphokinase, extensive macrophage infiltrates (labeled by RAM11) surrounding the necrotic muscle due to cholesterol crystals (labeled with Bopidy), with a concomitant increase in ^{18}F -FDG uptake.²⁴ In an accompanying editorial, Harikrishan et al elegantly reviewed the applications of ^{18}F -FDG-PET imaging in detecting myocardial inflammation, viability, vasculitis, and vulnerable plaques.²⁵ This study by Pervaiz et al adds another potential use for ^{18}F -FDG imaging of cholesterol crystal emboli-induced muscle and possibly other organ systems injury.²⁴

Last but not least, detection of prosthetic valve endocarditis using ^{18}F -FDG-PET imaging has been a success story with promising results. In a recent study, Saby et al studied 72 consecutive patients with suspicion of having prosthetic valve endocarditis with ^{18}F -FDG-

PET/CT. They reported sensitivity, specificity, positive predictive value, negative predictive value, and diagnostic accuracy of 73, 80, 85, 67, and 76%, respectively. Adding abnormal 18F-FDG-PET/CT imaging around the prosthetic valve as a major criterion significantly reduced the uncertain cases from 40 to 23, increased the sensitivity of the modified Duke criteria at admission from 70% to 97%, without comprising the specificity.²⁶

There has been however some debate whether late 18F-FDG imaging (150 min post injection) as opposed to conventional (60 min post injection) imaging might improve the diagnostic accuracy of the test. Scholtens et al showed that while conventional imaging yielded 1 false positive and 1 false negative out of 13 patients with suspected prosthetic valve endocarditis, late imaging resulted in 5 false-positive scans.²⁷ Early postoperative inflammation around the sewing ring of the prosthetic valve, unsuccessful suppression of myocardial FDG uptake, mild foreign body reaction around the prosthetic valve, atrial fibrillation, and overactive atrial myocytes, all are potential causes of false-positive scans, as outlined in the editorial by Schindler et al.²⁸ “Further improvements in dietary preparation in conjunction with several time points in FDG-PET/CT image acquisition may lead to a further refinement and improved diagnostic accuracy of 18F-FDG-PET/CT in the identification of prosthetic valve endocarditis”.²⁸

HEART FAILURE

There has been increasing research and interest in expanding the role of nuclear imaging in early detection of heart failure, characterizing different cardiomyopathy, guiding, and tailoring treatment accordingly. Within this scope, recent interest in myocardial efficiency has emerged. It is defined as the amount of external work (or pressure) that is created, relative to the amount of energy (or oxygen) that is consumed. The failing heart is inherently ineffective; it is unable to maintain stroke volume without inappropriate increase in filling pressures.²⁹ Early detection and interrogation of myocardial efficiency has potential value in the tailored management of heart failure. Measurement of myocardial efficiency is traditionally assessed invasively through pressure-volume loops. In an effort to establish non-invasive estimates of myocardial efficiency, 11C-acetate PET has emerged as a key technique.

This tracer is taken up by the myocardium in proportion to myocardial blood flow, transformed into 11C-acetyl-CoA, enters the tricarboxylic acid cycle, gets metabolized to carbon dioxide, and hence reflects the oxidative metabolism and oxygen consumption, with good reproducibility.³⁰ In parallel, workload is measured through the product of forward cardiac output

from early first pass phase of dynamic PET and systemic pressure. Indeed, Harms et al tested this approach in healthy controls and patients with valvular disease. Data on cardiac output and left ventricular mass were obtained from dynamic PET and re-measured with CMR. There was very good correlation of myocardial efficiency measurement using 11C-acetate PET dynamic imaging alone versus hybrid PET/CMR, and the technique was sensitive enough to detect subtle abnormalities in myocardial efficiency.³¹ The technique also exhibited excellent test-retest repeatability and operator reproducibility in another study by the same group.³² This non-invasive, reproducible, repeatable, and quantifiable method of assessing myocardial efficiency, without the need of other concomitant imaging modality, might play a significant role “of individually tailored, efficiency-guided medical heart failure therapy in the clinics,” as described by Bengel et al in an accompanying editorial.³³

Patients with diabetes often develop diastolic dysfunction and changes in myocardial metabolism with decrease in myocardial glucose uptake.³⁴ Impaired diastolic function is associated with worse outcomes.^{35–37} Whether such changes occur in the pre-diabetic state and in patients with reduced ejection fraction is not well established. Nielsen et al evaluated 35 patients with heart failure and reduced ejection fraction without diabetes and showed reduced myocardial glucose uptake among those with insulin resistance (i.e., pre-diabetic state) as compared to those with normal glucose tolerance, and despite normal myocardial blood flow.³⁸ Hence, changes in myocardial glucose uptake and metabolism start early in the pre-diabetic state, independent of myocardial blood flow. However, it is not clear whether whole-body insulin resistance causes direct myocardial insulin resistance, or whether heart failure induces both. Still, it is important to determine whether assessment of myocardial insulin resistance might help risk stratify patients, and whether early normalization of myocardial glucose uptake and metabolism improves outcomes.³⁹

Cardiac sarcoidosis often results in cardiomyopathy, heart failure, and arrhythmia.⁴⁰ Early detection of sarcoid nodules in the myocardium is important for early disease diagnosis, monitoring disease progression and response to treatment.^{18–20} 18F-FDG-PET imaging can detect inflammation; CMR detects tissue edema with T2 imaging, and scar formation with late Gadolinium enhancement. Hence, hybrid imaging with PET/CMR provides full morphological and complementary data for patients with cardiac sarcoidosis, as recently shown in a case series by Zandieh et al.⁴¹

Takotsubo cardiomyopathy is another form of dilated cardiomyopathy, often reversible, characterized

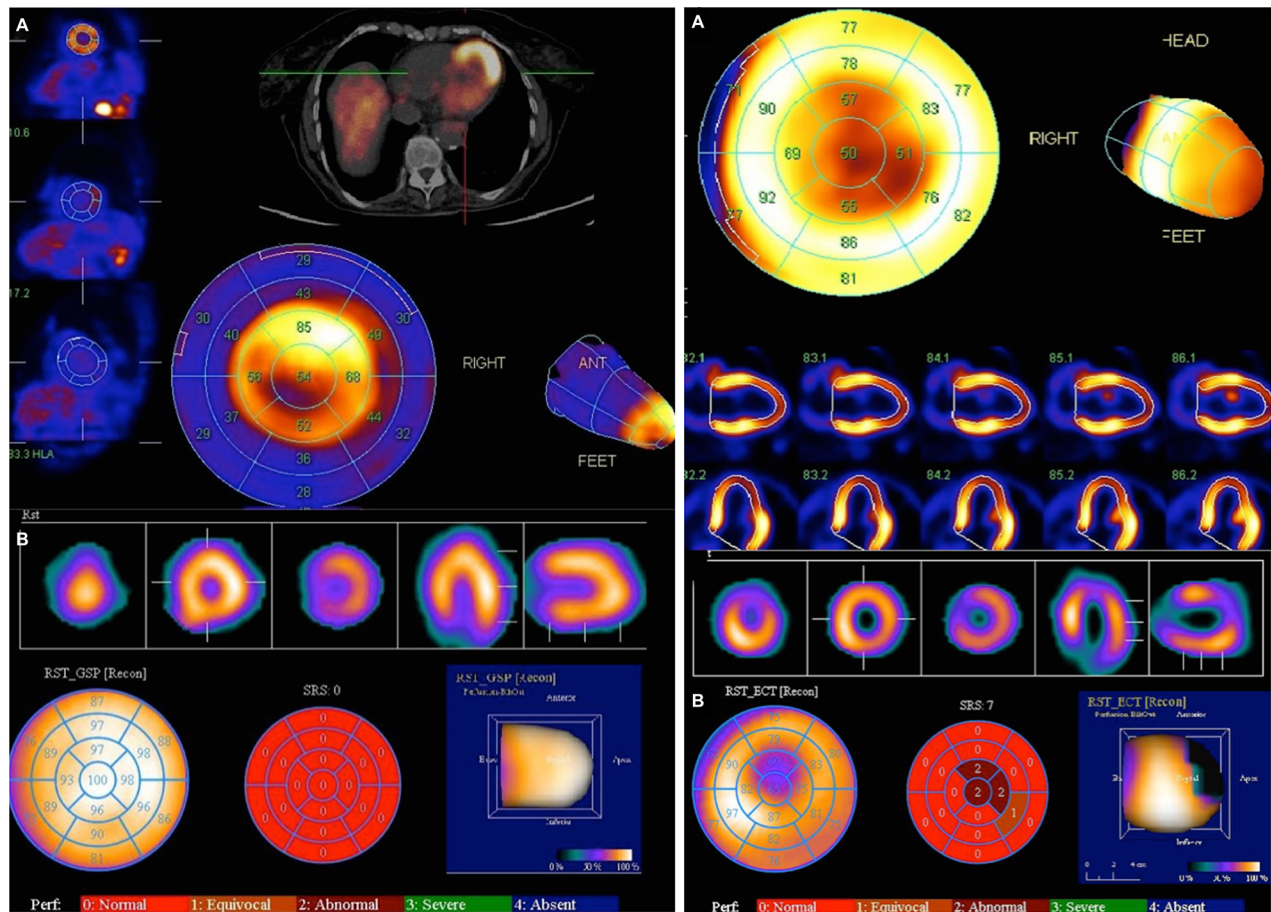


Figure 3. Illustrative cases of two patients with Takotsubo cardiomyopathy and wall motion abnormalities. The first case (left image) is characterized by apical hypermetabolism (high ^{18}F -FDG uptake, **A**) and normal perfusion with $^{99\text{m}}\text{Tc}$ -MIBI SPECT (**B**). The second case (right image) is characterized by decreased metabolism of the apical myocardium (**A**) and decreased perfusion (**B**). Reproduced with permission from Kobylecka et al⁴².

by significant regional wall motion abnormalities of mid and apical walls with compensatory hyperdynamic contraction of the basal walls. Kobylecka and colleagues from the Medical University of Warsaw studied the ^{18}F -FDG cardiac uptake pattern in 18 fasting patients with takotsubo cardiomyopathy and correlated the results with $^{99\text{m}}\text{Tc}$ -MIBI perfusion scintigraphy and echocardiography.⁴² Two distinct perfusion/metabolism patterns were detected: the first involving 8/18 patients characterized by apical hypermetabolism and normal perfusion in 7/8 patients; the second involving the remaining 10/18 patients characterized by decreased apical ^{18}F -FDG uptake in the apical myocardium with preserved activity elsewhere, and decreased perfusion in the majority of this subgroup⁴² (Figure 3). The different perfusion/metabolism patterns likely reflect different disease severities such as transient vasospasm with rapid recovery among those with apical

hypermetabolism, versus delayed recovery among those with relatively reduced apical metabolism. Whether this difference in perfusion/metabolic pattern actually impacts left ventricular function recovery, risks stratify patients, and predicts outcomes, needs further investigation in large prospective studies.⁴³

Cardiac amyloidosis is another intriguing form of cardiomyopathy. Early detection and differentiation of different subtypes has evolved over the last decade due to advancement in multi-modality imaging.⁴⁴ Transthyretin amyloid has a greater affinity for calcium as compared to primary amyloidosis; hence, the idea of using a bone tracer with SPECT imaging has re-emerged and was substantiated in multiple studies, showing high specificity of the tracer uptake for transthyretin amyloid.⁴⁴ Unlike other imaging modalities, nuclear imaging was the one capable of differentiating different types of amyloid. However, quantification of transthyretin

amyloid remained a challenge with SPECT imaging, and only qualitative grading is currently used. Given the higher spatial resolution, robust attenuation correction, superior count statistics, and the use of SUV, PET imaging could have an edge over SPECT imaging.⁴⁵ Indeed, the introduction of ¹⁸F-NaF, a PET tracer with affinity to calcium (used successfully to image microcalcification in plaques),¹¹ would theoretically bind more to transthyretin amyloidosis versus primary, similar to ^{99m}Tc-pyrophosphate. Morgenstern et al⁴⁶ showed that this tracer successfully differentiated the types of amyloidosis, and could be semi-quantitated as well. Another PET utilizing ¹¹C-Pittsburgh compound B was also tested and showed promising results in differentiating type B (only full length fibrils) versus type A (both fragmented and full length fibrils) transthyretin amyloid.⁴⁷ Quantification using SUV remains challenging, as previously experienced in oncology field, and several shortcomings of SUV measurement remain to be improved and overcome.⁴⁵

CORONARY ARTERY DISEASE

Among patients presenting with ST-elevation myocardial infarction, early revascularization translates into smaller infarct size, preserved viable myocardium, better ventricular function, and improved outcomes. While SPECT and CMR are frequently used to determine area at risk, infarct size, and myocardial salvage index, myocardial PET imaging can theoretically provide a comprehensive anatomical and functional evaluation in one single study to assess all of the above in addition to myocardial blood flow and reserve. In a recent study, Ghotbi et al compared the efficacy of ⁸²Rubidium PET to SPECT and CMR in patients with ST-elevation myocardial infarction without a prior history of myocardial infarction or coronary artery bypass surgery who underwent primary percutaneous coronary intervention.⁴⁸ Imaging was performed post-reperfusion and at a 3-month follow-up. An automated algorithm determined area at risk, final infarct size, and myocardial salvage index. While final infarct size and myocardial salvage index were comparable between modalities, there was significant variability among those with larger infarct size with PET imaging. Also, PET imaging underestimated area at risk by 7%.⁴⁸ Identifying a gold standard remains debatable. Additional unanswered questions includes identifying optimal cut-offs for area at risk, ideal PET tracer (⁸²Rb, ¹³N-NH₃, ¹⁸F-FDG, ¹⁸F-Flurpiridaz), and most cost-effective modality.⁴⁹

Identification of new PET tracer to detect myocardial injury and post-infarct remodeling is ongoing. ⁶⁸ Gallium-DOTA-peptide targets matrix metalloproteinases 2 and 9 that plays a role in extracellular

matrix remodeling post-myocardial injury. While Kiugel et al showed increased tracer activity in damaged myocardium using animal model, the tracer was unstable, rapidly metabolized, and slowly cleared in vivo, making it unsuitable for further evaluation.⁵⁰

While remote ischemic conditioning confers protection against myocardial ischemia-reperfusion injury and may modulate coronary blood flow, the effect on myocardial perfusion in patients with suspected coronary artery disease (CAD) is not well defined. Pryds et al tested the effect of remote ischemic conditioning in 49 patients with suspected ischemic CAD using ⁸²Rb-PET imaging.⁵¹ Ischemic conditioning was performed using four cycles of 5 minutes upper arm ischemia and reperfusion. MicroRNA-144 plasma levels were also measured before and after intervention. Unfortunately, there was no significant effect on resting global myocardial perfusion, in non-ischemic or ischemic myocardial territories.⁵¹

Patients with obstructive CAD also have myocardium at risk. Using invasive coronary angiogram as the reference standard, myocardium at risk as the quantitative parameter, and area under the curve as diagnostic performance index, Piccinelli et al showed that myocardial perfusion imaging (MPI)-CT angiogram fusion imaging provided incremental diagnostic information compared to MPI or CT angiogram alone for the diagnosis and localization of CAD.⁵² Quantitative hybrid imaging, which is a unique aspect of the study as compared to existing literature (mainly qualitative), has the potential to simplify the interpretation of multimodality cardiac imaging. Still, several steps were manually performed. Fully automated hybrid imaging, and integration of other parameters such as CT-fractional flow reserve, plaque burden, and others, could potentially enhance the diagnostic performance of hybrid SPECT MPI-CT angiogram.⁵³ Also, substituting SPECT by PET has additional advantages beyond improved spatial resolution including robust quantification of myocardial blood flow using dynamic imaging. In a recent study, Giubbini et al showed good correlation between summed difference score (ischemic burden) with ¹³N-NH₃ PET imaging and regional difference in myocardial blood flow (stress-rest).⁵⁴ There was, however, significant discordance in multiple vascular territories. Granted that there was no gold reference, such discordance might suggest “complementary information that may improve detection of obstructive CAD when the two measurements are combined” as nicely put by Sharir et al in an accompanying editorial.⁵⁵

Finally, the association between stress myocardial blood flow, myocardial perfusion reserve, and ventricular function was tested by Juarez-Orozo et al in 248 patients with suspected coronary ischemia undergoing

adenosine stress $^{13}\text{N-NH}_3$ PET imaging.⁵⁶ Stress myocardial blood flow outperformed perfusion reserve in determining ventricular function (systolic, diastolic, and synchrony-entropy).⁵⁶ This remained true whether patients had prior infarcted myocardium or not. Taking these findings a step further, a threshold value of stress myocardial blood flow that identifies abnormal perfusion and predicts left ventricular dysfunction should be defined. Also, the possibility of performing stress-only protocols by PET measuring peak stress myocardial blood flow and peak stress ventricular function can simplify the protocol, save time, costs, and limit radiation exposure.⁵⁷

COMPUTED TOMOGRAPHY

CT coronary angiography is commonly performed to assess coronary artery calcium (CAC) score and to visualize coronary anatomy for risk stratification. Indeed, a negative coronary CT angiogram has a pooled negative predictive value of 96% for cardiovascular events as shown in a recent meta-analysis of more than 6000 patients.⁵⁸ Meta-analyses, however, should be critically appraised to make sure the data were unbiased, and that rigorous methodology and analysis were used.⁵⁹ Also, additional data can be obtained from coronary CT angiography with additive prognostic value. Significant coronary artery stenosis can result in compromised resting perfusion abnormalities, which could be detected with CT perfusion imaging. In fact, using a computational algorithm trained by machine learning methods, Han et al showed that resting myocardial CT perfusion, improved discrimination (AUC increased from 0.68 to 0.75, $P = 0.001$) and reclassification (net reclassification index 0.52, $P < 0.001$) for ischemia as compared to CT angiography alone (invasive fractional flow reserve cut-off value < 0.80 as gold standard for ischemia).⁶⁰

The long-term prognostic value of coronary CT angiography, CAC score, and stress SPECT MPI was recently assessed in 164 patients with suspected CAD.⁶¹ While, CAC score, CT angiogram, and MPI were individually predictors of cardiac events, coronary CT angiography did not provide incremental prognostic information after combining CAC score and MPI findings with clinical data. Also, there were no events among those with CAC score of zero.⁶¹ The study however was limited by the small sample size, consisting of predominately low-risk asymptomatic patients, and excluding functional capacity from the analysis.⁶²

CT attenuation correction maps during PET imaging provides data on CAC score that are easily detected and manually categorized as mild, moderate, or severe. A developed machine learning algorithm could also potentially quantify the calcium score in an automated

manner. Isgum et al⁶³ sought to investigate whether such automated quantification would provide same cardiovascular risk stratification as standard manual categorization in 133 patients undergoing ^{82}Rb PET/CT imaging. Dedicated CT CAC score was performed on all patients and used as reference. There was strong agreement in cardiovascular disease risk categorization between manual and automatic scoring in CT attenuation correction at rest and stress (Cohen's linearly weighted κ of 0.85 and 0.89, respectively).⁶³ This study highlights the potential use of automatic CAC score method from the attenuation maps, sparing additional need dedicated CT and radiation, and perhaps widening its application to a variety of non-gated non-contrast CT scans. However, in a detailed editorial, Dumeer et al questioned the readiness of this software for prime time, at least not before achieving accuracy and workflow similar to manual and visual scoring, and performing validation study in multicenter settings with different vendor acquisitions.⁶⁴

Atherosclerosis is often detected on arterial beds such as thoracic aorta and other vessels, in addition to coronary arteries. These are easily identified on non-contrast CT scan. There is also increasing evidence that atherosclerosis starts in major vessel beds, predating coronary calcification. Allam et al performed total body non-contrast CT scan in 154 Egyptian patients (mean age 53 years) without known CAD and with normal MPI.⁶⁵ There was calcification in at least one vascular bed in 75% of patients, involving the iliofemoral (62%), abdominal aorta (53%), thoracic aorta (47%), carotids (25%), and coronary (47%) vascular beds. Among those with CAC score zero, calcification was present in 42%, 36%, 29%, and 7% of these vascular beds, respectively.⁶⁵ Hence, atherosclerotic calcifications are most common in the iliofemoral arteries and abdominal aorta, and likely predate coronary calcifications and myocardial ischemia (although serial studies in the same patients are not available for definitive conclusions) (Figure 4). An imaging strategy to detect and screen for extra-coronary atherosclerosis should be developed to better understand natural history of this disease and guide preventive strategies.

With all CT imaging, whether dedicated coronary or attenuation correction, extracardiac findings are often detected, necessitating additional investigation, and leading to further downstream resource utilization.⁶⁶ While many are benign, some are clinically significant. Indeed, Zadro et al showed in a retrospective study of 1506 patients, more than half of patients had minor and 14% had major extracardiac findings.⁶⁷ The latter was associated with poor mid-term survival, irrespective of the perfusion results. Given the significant impact of major extracardiac findings on survival, regardless of

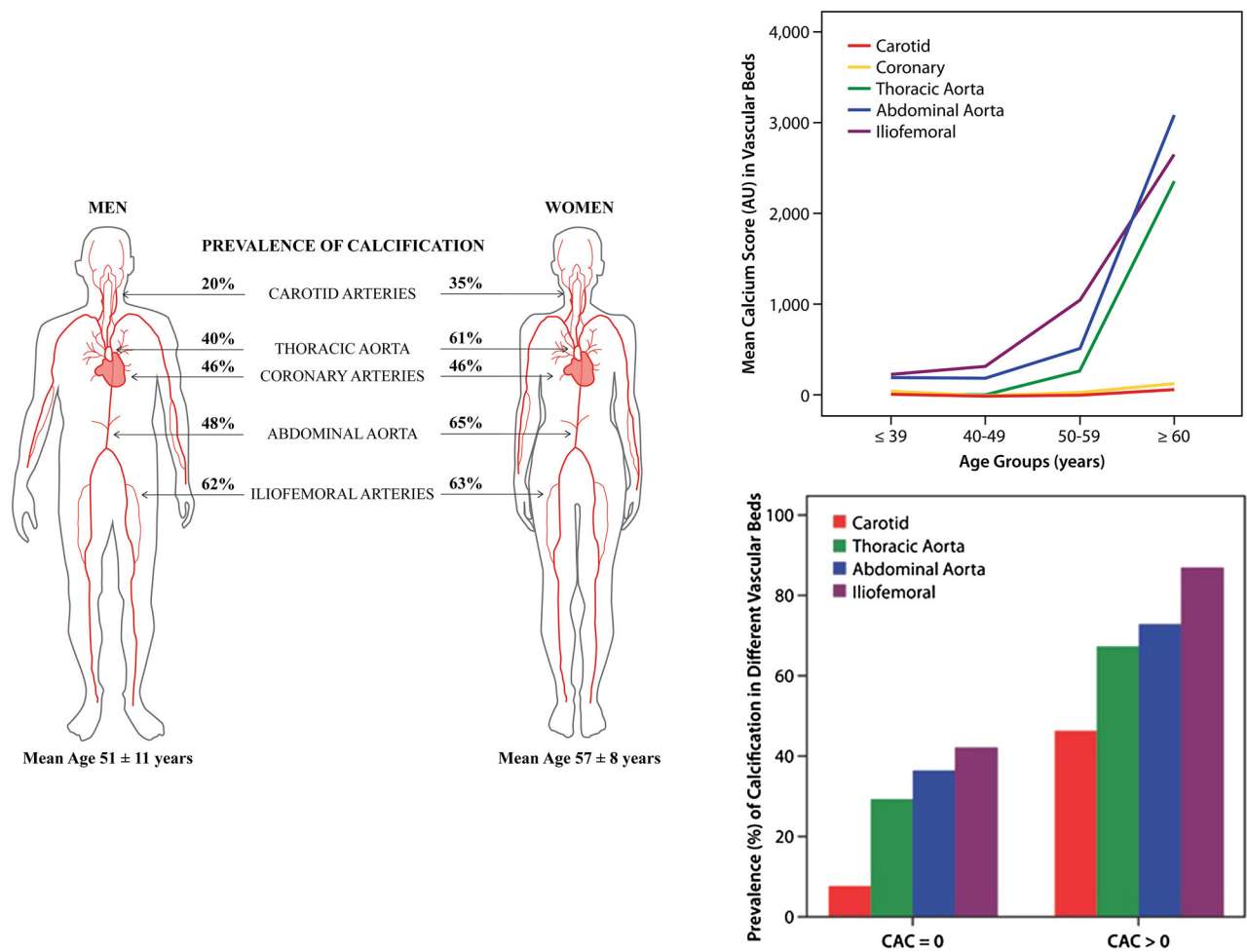


Figure 4. Prevalence of extra-coronary artery calcification stratified by gender, age, and presence or absence of coronary artery calcification. Reproduced with permission from Allam et al⁶⁵.

perfusion results, any downstream testing theoretically might outweigh potential associated risk of physical harm and additional cost. Most importantly, accurate assessment and reporting of extracardiac findings should occur after interdisciplinary discussion with the referring physician taking into account clinical background and risk factors, as pointed out by Dominik et al in an accompanying editorial.⁶⁸

TECHNICAL ASPECT OF IMAGING

The constant advancement in the cardiology field of PET imaging is not possible without a parallel improvement in the technical aspect of patient preparation, image acquisition, or post-processing. For example, one of the major drawbacks of cardiac sarcoid nodule imaging with 18F-FDG-PET is lack of suppression of normal myocardium glucose uptake; this results in false-positive or uninterpretable study. While high fat diet

followed by prolonged fasting is critical for performing these studies, an unacceptably high rate of lack of suppression persists with dietary preparation alone.⁶⁹ Prior studies have demonstrated the potential benefit of unfractionated heparin as an add-on to dietary preparation. Giorgetti et al showed that other anticoagulants such as warfarin and low-molecular weight heparin can be used successfully to adequately suppress the glucose metabolism of healthy myocardium.⁷⁰ The study, however, did not include patients on direct oral anticoagulant, which are now commonly used as alternative to heparin and warfarin for various clinical indications. It is important to assess whether such drugs can also achieve similar myocardial glucose suppression. Still, no single protocol has achieved 100% suppression of physiological 18F-FDG myocardial uptake, or significant superiority compared to others.⁷¹ Additional research and technique optimization are still needed.

Quantification of myocardial blood flow with dynamic PET imaging is used increasingly to diagnose multi-vessel and micro-vascular CAD.⁷² However, variability in the measurements may introduce errors and affect clinical decision. In an effort to improve test-retest repeatability of myocardial blood flow quantification, Klein et al evaluated the effects of ⁸²Rb tracer injection profile using a constant-activity-rate versus a constant-flow-rate infusion; the former technique produced more repeatable tracer injection profiles, decreased the test-retest variability of flow measurements, without affecting perfusion image quality.⁷³ “When integrating myocardial blood flow measurements into practice, it is vitally important that all of the clinical staff be trained on the entire protocol, including patient preparation, vasodilator stressing, imaging parameters, quality control, processing, and interpretation.”⁷⁴

Furthermore, the effect of prompt gamma compensation, an algorithm that is routinely implemented by the manufacturer of most state of the art 3D-PET scanner, on myocardial blood flow is not well established. Armstrong et al recently showed that such algorithm causes significant changes in myocardial blood flow, particularly in the left anterior descending and circumflex coronary arteries of obese patients.⁷⁵ However, since the changes affect both stress and rest flow evenly, the myocardial flow reserve is not significantly altered. Still, proper awareness of prompt gamma compensation on myocardial blood flow is of crucial importance.⁷⁶

Cardiac and respiratory motion is not an uncommon source of artifact and suboptimal images in patients undergoing PET imaging. Adenosine infusion in particular, during pharmacological stress testing, is associated with significantly more cardiac motion as compared to regadenoson, due to a drift of the heart away from baseline position, coinciding with the termination of the infusion.⁷⁷ The impact of such drift, on perfusion images, diagnostic accuracy of the test, and quantitative blood flow analysis was not assessed. Also, the study lacked internal control with crossover-blinded design study.⁷⁸ Further research to determine the clinical significance of this finding, and whether corrective measures that might add time and complexity to PET imaging, is needed.

Respiratory motion can also impact image quality. Ischikawa assessed the usefulness of abdominal belt for restricting respiratory cardiac motion and improving image quality in myocardial perfusion PET.⁷⁹ The belt technique was well tolerated, improved image quality without adverse events. Alternative respiratory motion correction techniques include using a data-driven self-gating technique to gate the PET activities into multiple bins over a respiratory cycle without any hardware

gating. Whether such techniques have clinical-proven benefit to patients needs to be assessed as they add time and complexity to data acquisition and post-processing.⁸⁰

Finally, the effect of advanced image correction techniques with time-of-flight and point spread function modeling in image reconstruction were recently studied by Dasari et al in 36 obese patients undergoing ⁸²Rb-PET imaging.⁸¹ Time-of-flight modeling decreased summed stress and rest score equally without change in summed difference score, while point spread function had negligible effect on all 3 perfusion parameters. The study highlights that different image post-processing algorithms affect perfusion defect sizes; however, in the absence of a gold standard or phantom reference, it is not clear whether the smaller perfusion defect sizes with time-of-flight reconstruction are the correct ones or just underestimated. Also, all data originate from one single vendor and cannot be extrapolated to other vendor PET in the market.^{82,83} The impact of different vendors and software on perfusion defect size and other quantitative left ventricular parameters was previously assessed by our group, and was not negligible.⁸⁴ There is much need for a phantom reference for calibration of all quantifiable parameters, and ensuring good inter-vendor reproducibility.

Each year, new discoveries and exciting research emerge in the field of nuclear cardiology. The current review was an attempt to summarize several key articles related to PET, CT, and CMR imaging that were published last year in the Journal of Nuclear Cardiology. Unfortunately, there were several other interesting and relevant papers that we could not discuss due to space constraint, and we apologize for that. The next part of this review will summarize the key articles in SPECT imaging. We look forward to next year’s publications and discoveries.

Disclosures

Dr. Hage reports research support from Astellas Pharma and GE Healthcare. Dr. AlJaroudi reports no conflicts of interest.

References

1. AlJaroudi WA, Hage FG. Review of cardiovascular imaging in the journal of nuclear cardiology in 2014: Part 1 of 2: Positron emission tomography, computed tomography, and neuronal imaging. *J Nucl Cardiol* 2015;22:507-12.
2. Hage FG, AlJaroudi WA. Review of cardiovascular imaging in the journal of nuclear cardiology in 2014: Part 2 of 2: Myocardial perfusion imaging. *J Nucl Cardiol* 2015;22:714-9.

3. AlJaroudi WA, Hage FG. Review of cardiovascular imaging in the journal of nuclear cardiology in 2015. Part 1 of 2: Plaque imaging, positron emission tomography, computed tomography, and magnetic resonance. *J Nucl Cardiol* 2016;23:122-30.
4. Hage FG, AlJaroudi WA. Review of cardiovascular imaging in the journal of nuclear cardiology in 2015-part 2 of 2: Myocardial perfusion imaging. *J Nucl Cardiol* 2016;23:493-8.
5. AlJaroudi W, Hage FG. Review of cardiovascular imaging in the journal of nuclear cardiology in 2016. Part 1 of 2: Positron emission tomography, computed tomography and magnetic resonance. *J Nucl Cardiol* 2017;24:649-56.
6. Hage FG, AlJaroudi WA. Review of cardiovascular imaging in the journal of nuclear cardiology in 2016: Part 2 of 2-myocardial perfusion imaging. *J Nucl Cardiol* 2017;24:1190-9.
7. AlJaroudi WA, Hage FG. Review of cardiovascular imaging in the journal of nuclear cardiology 2017 Part 1 of 2: Positron emission tomography, computed tomography, and magnetic resonance. *J Nucl Cardiol* 2018;25:320-30.
8. Hage FG, AlJaroudi WA. Review of cardiovascular imaging in the journal of nuclear cardiology in 2017 Part 2 of 2: Myocardial perfusion imaging. *J Nucl Cardiol* 2018;25:1390-9.
9. Bentzon JF, Otsuka F, Virmani R, Falk E. Mechanisms of plaque formation and rupture. *Circ Res* 2014;114:1852-66.
10. Tarkin JM, Rudd JH. Techniques for noninvasive molecular imaging of atherosclerotic plaque. *Nat Rev Cardiol* 2015;12:79.
11. Li X, Heber D, Cal-Gonzalez J, Karanikas G, Mayerhoefer ME, Rasul S, et al. Association between osteogenesis and inflammation during the progression of calcified plaque evaluated by (18)f-fluoride and (18)f-fdg. *J Nucl Med* 2017;58:968-74.
12. Ferreira MJV, Oliveira-Santos M, Silva R, Gomes A, Ferreira N, Abruñhosa A, et al. Assessment of atherosclerotic plaque calcification using f18-naf pet-ct. *J Nucl Cardiol* 2018;25:1733-41.
13. Marchesseau S, Seneviratna A, Sjöholm AT, Qin DL, Ho JXM, Hausenloy DJ, et al. Hybrid pet/ct and pet/mri imaging of vulnerable coronary plaque and myocardial scar tissue in acute myocardial infarction. *J Nucl Cardiol* 2017;25:1-11.
14. Moustafa A, Abi-Saleh B, El-Baba M, Hamoui O, AlJaroudi W. Anatomic distribution of culprit lesions in patients with non-st-segment elevation myocardial infarction and normal eeg. *Cardiovasc Diagn Ther* 2016;6:25-33.
15. Cal-Gonzalez J, Li X, Heber D, Rausch I, Moore SC, Schafers K, et al. Partial volume correction for improved pet quantification in (18)f-naf imaging of atherosclerotic plaques. *J Nucl Cardiol* 2018;25:1742-56.
16. Alavi A, Werner TJ, Hoiland-Carlson PF. What can be and what cannot be accomplished with pet to detect and characterize atherosclerotic plaques. *J Nucl Cardiol* 2017;25:12-5.
17. Tavakoli S, Vashist A, Sadeghi MM. Molecular imaging of plaque vulnerability. *J Nucl Cardiol* 2014;21:1112-28.
18. Manabe O, Ohira H, Hirata K, Hayashi S, Naya M, Tsujino I, et al. Use of (18)f-fdg pet/ct texture analysis to diagnose cardiac sarcoidosis. *Eur J Nucl Med Mol Imaging* 2018. <https://doi.org/10.1007/s00259-018-4195-9>.
19. Braun JJ, Kessler R, Constantinesco A, Imperiale A. 18f-fdg pet/ct in sarcoidosis management: Review and report of 20 cases. *Eur J Nucl Med Mol Imaging* 2008;35:1537-43.
20. Wada K, Niitsuma T, Yamaki T, Masuda A, Ito H, Kubo H, et al. Simultaneous cardiac imaging to detect inflammation and scar tissue with (18)f-fluorodeoxyglucose pet/mri in cardiac sarcoidosis. *J Nucl Cardiol* 2016;23:1180-2.
21. Nensa F, Kloth J, Tezgaeh E, Poepfel TD, Heusch P, Goebel J, et al. Feasibility of fdg-pet in myocarditis: Comparison to cmr using integrated pet/mri. *J Nucl Cardiol* 2018;25:785-94.
22. Rischpler C, Langwieser N, Nekolla SG. Cardiac pet/mri enters the clinical arena! Finally. *J Nucl Cardiol* 2018;25:795-6.
23. Tarkin JM, Joshi FR, Rudd JH. Pet imaging of inflammation in atherosclerosis. *Nat Rev Cardiol* 2014;11:443-57.
24. Pervaiz MH, Durga S, Janoudi A, Berger K, Abela GS. Pet/cta detection of muscle inflammation related to cholesterol crystal emboli without arterial obstruction. *J Nucl Cardiol* 2018;25:433-40.
25. Harikrishnan P, Gerard P, Jain D. (18)f-fdg for imaging microvascular injury. *J Nucl Cardiol* 2018;25:441-2.
26. Saby L, Laas O, Habib G, Cammilleri S, Mancini J, Tessonnier L, et al. Positron emission tomography/computed tomography for diagnosis of prosthetic valve endocarditis: Increased valvular 18f-fluorodeoxyglucose uptake as a novel major criterion. *J Am Coll Cardiol* 2013;61:2374-82.
27. Scholtens AM, Swart LE, Verberne HJ, Budde RPJ, Lam M. Dual-time-point fdg pet/ct imaging in prosthetic heart valve endocarditis. *J Nucl Cardiol* 2017;25:1960-7.
28. Schindler TH. Another potential step to improve prosthetic heart valve endocarditis imaging with (18)f-fdg pet/ct. *J Nucl Cardiol* 2017;25:1968-70.
29. Knaepen P, Germans T, Knuuti J, Paulus WJ, Dijkmans PA, Allaart CP, et al. Myocardial energetics and efficiency: Current status of the noninvasive approach. *Circulation* 2007;115:918-27.
30. Nesterov SV, Turta O, Han C, Maki M, Lisinen I, Tuunanen H, et al. C-11 acetate has excellent reproducibility for quantification of myocardial oxidative metabolism. *Eur Heart J Cardiovasc Imaging* 2015;16:500-6.
31. Harms HJ, Hansson NHS, Kero T, Baron T, Tolbod LP, Kim WY, et al. Automatic calculation of myocardial external efficiency using a single (11)c-acetate pet scan. *J Nucl Cardiol* 2018;25:1937-44.
32. Wu KY, Dinculescu V, Renaud JM, Chen SY, Burwash IG, Mielniczuk LM, et al. Repeatable and reproducible measurements of myocardial oxidative metabolism, blood flow and external efficiency using (11)c-acetate pet. *J Nucl Cardiol* 2018;25:1912-25.
33. Bengel FM. Pet-based myocardial efficiency: Powerful yet underutilized-now simpler than ever. *J Nucl Cardiol* 2018;25:1945-7.
34. Hu L, Qiu C, Wang X, Xu M, Shao X, Wang Y. The association between diabetes mellitus and reduction in myocardial glucose uptake: A population-based (18)f-fdg pet/ct study. *BMC Cardiovasc Disord* 2018;18:203.
35. Aljaroudi W, Alraies MC, Halley C, Rodriguez L, Grimm RA, Thomas JD, et al. Impact of progression of diastolic dysfunction on mortality in patients with normal ejection fraction. *Circulation* 2012;125:782-8.
36. AlJaroudi WA, Thomas JD, Rodriguez LL, Jaber WA. Prognostic value of diastolic dysfunction: State of the art review. *Cardiol Rev* 2014;22:79-90.
37. AlJaroudi WA, Alraies MC, Halley C, Menon V, Rodriguez LL, Grimm RA, et al. Incremental prognostic value of diastolic dysfunction in low risk patients undergoing echocardiography: Beyond framingham score. *Int J Cardiovasc Imaging* 2013;29:1441-50.
38. Nielsen R, Jorsal A, Iversen P, Tolbod L, Bouchelouche K, Sorensen J, et al. Heart failure patients with prediabetes and newly diagnosed diabetes display abnormalities in myocardial metabolism. *J Nucl Cardiol* 2018;25:169-76.
39. Gargiulo P, Perrone-Filardi P. Heart failure, whole-body insulin resistance and myocardial insulin resistance: An intriguing puzzle. *J Nucl Cardiol* 2018;25:177-80.
40. Patel MR, Cawley PJ, Heitner JF, Klem I, Parker MA, Jaroudi WA, et al. Detection of myocardial damage in patients with sarcoidosis. *Circulation* 2009;120:1969-77.

41. Zandieh S, Bernt R, Mirzaei S, Haller J, Hergan K. Image fusion between 18f-fdg pet and mri in cardiac sarcoidosis: A case series. *J Nucl Cardiol* 2018;25:1128-34.
42. Kobylecka M, Budnik M, Kochanowski J, Piatkowski R, Chojnowski M, Fronczewska-Wieniawska K, et al. Takotsubo cardiomyopathy: Fdg myocardial uptake pattern in fasting patients. Comparison of pet/ct, spect, and echo results. *J Nucl Cardiol* 2018;25:1260-70.
43. Bhambhani P. Under the hood of the stunned takotsubo heart. *J Nucl Cardiol* 2018;25:1271-3.
44. Aljaroudi WA, Desai MY, Tang WH, Phelan D, Cerqueira MD, Jaber WA. Role of imaging in the diagnosis and management of patients with cardiac amyloidosis: State of the art review and focus on emerging nuclear techniques. *J Nucl Cardiol* 2014;21:271-83.
45. Soman P, Masri A. Setting the stage for the next step in cardiac amyloidosis imaging: Serial quantitative studies to assess disease activity. *J Nucl Cardiol* 2018;25:1571-3.
46. Morgenstern R, Yeh R, Castano A, Maurer MS, Bokhari S. (18)fluorine sodium fluoride positron emission tomography, a potential biomarker of transthyretin cardiac amyloidosis. *J Nucl Cardiol* 2018;25:1559-67.
47. Pilebro B, Arvidsson S, Lindqvist P, Sundstrom T, Westermarck P, Antoni G, et al. Positron emission tomography (pet) utilizing pittsburgh compound b (pib) for detection of amyloid heart deposits in hereditary transthyretin amyloidosis (attr). *J Nucl Cardiol* 2018;25:240-8.
48. Ghotbi AA, Kjaer A, Nepper-Christensen L, Ahtarovski KA, Lonborg JT, Vejstrup N, et al. Subacute cardiac rubidium-82 positron emission tomography ((82)rb-pet) to assess myocardial area at risk, final infarct size, and myocardial salvage after stemi. *J Nucl Cardiol* 2018;25:970-81.
49. Andrikopoulou E, Lloyd SG. Could (82)rb-pet be the next best thing in evaluation of myocardial salvage? *J Nucl Cardiol* 2018;25:982-5.
50. Kiugel M, Kyto V, Saanijoki T, Liljenback H, Metsala O, Stahle M, et al. Evaluation of (68)ga-labeled peptide tracer for detection of gelatinase expression after myocardial infarction in rat. *J Nucl Cardiol* 2018;25:1114-23.
51. Pryds K, Nielsen RR, Hoff CM, Tolbod LP, Bouchelouche K, Li J, et al. Effect of remote ischemic conditioning on myocardial perfusion in patients with suspected ischemic coronary artery disease. *J Nucl Cardiol* 2018;25:887-96.
52. Piccinelli M, Santana C, Sirineni GKR, Folks RD, Cooke CD, Arepalli CD, et al. Diagnostic performance of the quantification of myocardium at risk from mpi spect/cta 2g fusion for detecting obstructive coronary disease: A multicenter trial. *J Nucl Cardiol* 2018;25:1376-86.
53. Slomka P. Hybrid quantitative imaging: Will it enter clinical practice? *J Nucl Cardiol* 2018;25:1387-9.
54. Giubbini R, Peli A, Milan E, Sciaga R, Camoni L, Albano D, et al. Comparison between the summed difference score and myocardial blood flow measured by (13)n-ammonia. *J Nucl Cardiol* 2018;25:1621-8.
55. Sharir T, Kovalski G. Absolute myocardial blood flow vs relative myocardial perfusion: Which one is better? *J Nucl Cardiol* 2018;25:1629-32.
56. Juarez-Orozco LE, Alexanderson E, Dierckx RA, Boersma HH, Hillege JL, Zeebregts CJ, et al. Stress myocardial blood flow correlates with ventricular function and synchrony better than myocardial perfusion reserve: A nitrogen-13 ammonia pet study. *J Nucl Cardiol* 2018;25:797-806.
57. Giubbini R, Peli A. Left ventricular function during hyperemia: A dive into the unknown. *J Nucl Cardiol* 2018;25:807-8.
58. Green R, Cantoni V, Petretta M, Acampa W, Panico M, Buongiorno P, et al. Negative predictive value of stress myocardial perfusion imaging and coronary computed tomography angiography: A meta-analysis. *J Nucl Cardiol* 2018;25:1588-97.
59. Patel N, Bajaj NS. Meta-analyses: How to critically appraise them? *J Nucl Cardiol* 2018;25:1598-600.
60. Han D, Lee JH, Rizvi A, Gransar H, Baskaran L, Schulman-Marcus J, et al. Incremental role of resting myocardial computed tomography perfusion for predicting physiologically significant coronary artery disease: A machine learning approach. *J Nucl Cardiol* 2018;25:223-33.
61. Nappi C, Nicolai E, Daniele S, Acampa W, Gaudieri V, Assante R, et al. Long-term prognostic value of coronary artery calcium scanning, coronary computed tomographic angiography and stress myocardial perfusion imaging in patients with suspected coronary artery disease. *J Nucl Cardiol* 2018;25:833-41.
62. Robinson AA, Bourque JM. Combined non-invasive imaging for predicting cardiovascular events : Is three a crowd? *J Nucl Cardiol* 2018;25:842-4.
63. Isgum I, de Vos BD, Wolterink JM, Dey D, Berman DS, Rubeaux M, et al. Automatic determination of cardiovascular risk by ct attenuation correction maps in rb-82 pet/ct. *J Nucl Cardiol* 2017;25:2133-42.
64. Dumeer S, Einstein AJ. Coronary calcium scoring of ct attenuation correction scans: Automatic, manual, or visual? *J Nucl Cardiol* 2017;25:2144-7.
65. Allam AHA, Thompson RC, Eskander MA, Mandour Ali MA, Sadek A, Rowan CJ, et al. Is coronary calcium scoring too late? Total body arterial calcium burden in patients without known cad and normal mpi. *J Nucl Cardiol* 2017;25:1990-8.
66. Qureshi WT, Alirhayim Z, Khalid F, Al-Mallah MH. Prognostic value of extracardiac incidental findings on attenuation correction cardiac computed tomography. *J Nucl Cardiol* 2016;23:1266-74.
67. Zadro C, Roussel N, Cassol E, Pascal P, Petermann A, Meyrignac O, et al. Prognostic impact of myocardial perfusion single photon emission computed tomography in patients with major extracardiac findings by computed tomography for attenuation correction. *J Nucl Cardiol* 2018;25:1574-83.
68. Benz DC, Fuchs TA. Extracardiac findings on computed tomography attenuation correction: Is it worth paying extra attention? *J Nucl Cardiol* 2018;25:1584-7.
69. Manabe O, Yoshinaga K, Ohira H, Masuda A, Sato T, Tsujino I, et al. The effects of 18-h fasting with low-carbohydrate diet preparation on suppressed physiological myocardial (18)f-fluorodeoxyglucose (fdg) uptake and possible minimal effects of unfractionated heparin use in patients with suspected cardiac involvement sarcoidosis. *J Nucl Cardiol* 2016;23:244-52.
70. Giorgetti A, Marras G, Genovesi D, Filidei E, Bottoni A, Mangione M, et al. Effect of prolonged fasting and low molecular weight heparin or warfarin therapies on 2-deoxy-2-[18f]-fluoro-d-glucose pet cardiac uptake. *J Nucl Cardiol* 2018;25:1364-71.
71. Andrikopoulou E, Bhambhani P. Optimizing myocardial metabolism for fluorine-18 fluorodeoxyglucose positron emission tomography imaging of cardiac inflammation. *J Nucl Cardiol* 2018;25:1372-5.
72. Ziadi MC, Dekemp RA, Williams K, Guo A, Renaud JM, Chow BJ, et al. Does quantification of myocardial flow reserve using rubidium-82 positron emission tomography facilitate detection of multivessel coronary artery disease? *J Nucl Cardiol* 2012;19:670-80.
73. Klein R, Ocneanu A, Renaud JM, Ziadi MC, Beanlands RSB, deKemp RA. Consistent tracer administration profile improves test-retest repeatability of myocardial blood flow quantification with (82)rb dynamic pet imaging. *J Nucl Cardiol* 2018;25:929-41.

74. Case J. Accurate myocardial blood flow measurements: Quality from start to finish is key to success. *J Nucl Cardiol* 2018;25:942-6.
75. Armstrong IS, Memmott MJ, Tonge CM, Arumugam P. The impact of prompt gamma compensation on myocardial blood flow measurements with rubidium-82 dynamic PET. *J Nucl Cardiol* 2018;25:596-605.
76. Moncayo VM, Garcia EV. Prompt-gamma compensation in rb-82 myocardial perfusion 3d pet/ct: Effect on clinical practice. *J Nucl Cardiol* 2018;25:606-8.
77. Memmott MJ, Tonge CM, Saint KJ, Arumugam P. Impact of pharmacological stress agent on patient motion during rubidium-82 myocardial perfusion PET/CT. *J Nucl Cardiol* 2018;25:1286-95.
78. Cremer PC, DiFilippo FP, Jaber WA. Moving towards a better understanding of potential pitfalls in quantitative pet myocardial blood flow. *J Nucl Cardiol* 2018;25:1296-8.
79. Ichikawa Y, Tomita Y, Ishida M, Kobayashi S, Takeda K, Sakuma H. Usefulness of abdominal belt for restricting respiratory cardiac motion and improving image quality in myocardial perfusion pet. *J Nucl Cardiol* 2018;25:407-15.
80. Pan T. Respiratory gating in PET/CT: A step in the right direction. *J Nucl Cardiol* 2018;25:416-8.
81. Dasari PKR, Jones JP, Casey ME, Liang Y, Dilsizian V, Smith MF. The effect of time-of-flight and point spread function modeling on (82)rb myocardial perfusion imaging of obese patients. *J Nucl Cardiol* 2018;25:1521-45.
82. Armstrong IS. Understanding the impact of advanced pet reconstruction in cardiac PET: The devil is in the details. *J Nucl Cardiol* 2018;25:1546-9.
83. Matheoud R, Lecchi M, et al. Time-of-flight in cardiac PET/CT: What do we know and what we should know? *J Nucl Cardiol* 2018. <https://doi.org/10.1007/s12350-018-1336-2>.
84. Ather S, Iqbal F, Gulotta J, Aljaroudi W, Heo J, Iskandrian AE, et al. Comparison of three commercially available softwares for measuring left ventricular perfusion and function by gated SPECT myocardial perfusion imaging. *J Nucl Cardiol* 2014;21:673-81.